JOURNAL OF AIRCRAFT
Vol. 37, No. 3, May–June 2000

Universality of the Moving-Wall Effect

Lars E. Ericsson*
Mountain View, California 94040
and
Martin E. Beyers†
Institute for Aerospace Research, Ottawa, Ontario K1A 0R6, Canada

An analysis of published experimental results on the unsteady aerodynamics of separated flow has established that the importance of the moving-wall effect is not limited to two-dimensional dynamic airfoil stall. It plays an equally prominent role in the case of three-dimensional unsteady separated flow on a maneuvering combat aircraft. The moving-wall effect can remain effective in the presence of flow unsteadiness. However, when the flow unsteadiness causes bifurcation of the time-averaged flow, the moving-wall effect can be suppressed.

Introduction

REVIEWERS of two recent papers,[1,2] in which the unsteady high-alpha aerodynamics of combat aircraft was analyzed, expressed the opinion that the applied moving-wall effect[3] may not be the only flow mechanism that could explain the most unusual results obtained in rotary balance tests of a generic combat aircraft model.[4] The reviewers were also concerned that three-dimensional flow effects may have prevented the moving-wall effect from functioning as envisioned in Refs. 1 and 2. Another concern was that flow unsteadiness could make it difficult to correctly apply the steady moving-wall effect, which generates Magnus lift,[5] to describe the flow separation characteristics on a maneuvering combat aircraft. In response to these expressed concerns, a review and extension of earlier analyses employing the moving-wall effect has been undertaken. Care has been exercised to provide an explicit description of the flow physics in order to answer in a satisfactory manner the questions raised in regard to the veracity of this flow concept. Two-dimensional flow separation characteristics are discussed first before considering the complications added by three-dimensional flow effects.

Discussion

When and where flow separation occurs on an airfoil is determined by the boundary-layer profile shape and the adversity of the pressure gradient. The delay of stall through the dynamic effect of the airfoil motion on the pressure gradient can be determined by applying the unsteady Bernoulli equation.[6] Adding the pitch-rate-induced camber effect and the Karman–Sears wake lag gave satisfactory prediction[6] of the experimental results for the VERTOL 23010-1.58 airfoil[7] (Fig. 1). The satisfaction lasted until trying to apply the same analytic method to predict the experimental results[8] in Fig. 2. The accelerated flow effect $\Delta\alpha_S$ can only delay the occurrence of flow separation, whereas prediction of the experimental results in Fig. 2 requires a flow mechanism that can reattach fully separated flow. At $\alpha = 22$ deg, the airfoil is in the deep stall region, and the minimum angle of attack of the 6-deg amplitude oscillation is $\alpha = 16$ deg, still far above the static stall angle $\alpha \approx 10$ deg. As the data points in Fig. 2 represent the time-averaged values, it is clear from Fig. 1 that in Fig. 2 very high dynamic lift must have been generated during the upstroke.

A powerful flow mechanism that could produce this is the moving-wall effect[3,9,10] (Fig. 3). As the wing is pitching or plunging upward during the upstroke, the generated flow velocity at the leading edge surface has to be equal to the tangential velocity U_W of the airfoil surface to satisfy the no-slip condition. When the airflow has turned the corner to the upper surface of the airfoil, the tangential wall velocity decreases rapidly, and the near-wall boundary layer is left with an excess velocity. This motion-induced wall-jet effect improves the boundary-layer layer profile (Fig. 3a), delaying flow separation. On the downstroke the wall-jet effect generates a separation-prone profile, promoting flow separation (Fig. 3b). The effect can be visualized as the illustrated roller-like effect created by a rotating leading-edge cylinder of radius r_N.

Experiments[11,12] (Fig. 4) have shown that wall jets, which were too small to be traceable in the measured boundary-layer profile (at $s = 0.25$ IN), could eliminate the leading-edge separation bubble (at $s = 0.50$ IN). Thus, one could expect that the wall-jet-like moving-wall effect (Fig. 3) may be of sufficient magnitude to cause the large overshoot of static lift maximum required to produce the experimental results in Fig. 2. The measured boundary-layer profiles at $s = 0.25$ IN in Fig. 4 demonstrate the futility of trying to define the wall jet through standard boundary-layer profile measurements.[13] Measuring the moving-wall-induced wall-jet effect would be expected to be equally difficult, as $|U_W/U_\infty| = \xi_{CG}\bar{\omega}\Delta\theta = 0.008$ for $\bar{\omega} = 0.2$ in Fig. 2. It has been demonstrated that wall jets of minuscule strength can cause reattachment of fully separated flow.[14] Experimental results at $\alpha = 22$ deg for a NACA-0015 airfoil (Fig. 5) showed that a blowing-generated leading-edge jet could increase the maximum lift from $c_{l\max} = 0.68$ to $c_{l\max} \approx 1.2$ by using steady blowing of $c_\mu = 0.03$. When using oscillatory blowing/suction, only $\Delta c_\mu = 0.06\%$ was needed.

Extension to Three-Dimensional Flow

The preceding discussion shows that a viscous flow mechanism is needed in conjunction with the accelerated flow effect in order to predict the dynamic airfoil stall. In the presence of this viscous fluid/motion coupling, the stagnation point is displaced to satisfy the no-slip condition. This can be related to the delay $\Delta\alpha_S$ of the onset of stall discussed earlier, giving the following total delay of stall:

$$\Delta\alpha = \Delta\alpha_W + \Delta\alpha_S \tag{1}$$

where $\Delta\alpha_W$ is proportional to the leading-edge velocity $-\dot{z}_{LE}/U_\infty$ in the two-dimensional case discussed earlier. For the plunging leading edge the wall is subjected to opposite shear stresses on the upper and lower sides of the stagnation line. The resulting accelerated flow effect is accompanied by a change in flow curvature, generating the stall delay $\Delta\alpha_S$. However, it is the moving-wall effect $\Delta\alpha_W$ that

Presented as Paper 99-0647 at the 37th Aerospace Sciences Meeting and Exhibit (Oct), Reno, NV, 11–14 January 1999; received 4 May 1999; revision received 29 November 1999; accepted for publication 15 December 1999.

*Engineering Consultant. Fellow AIAA.
†Head, Aircraft Aerodynamics Group, Aerodynamics Laboratory. Senior Member AIAA.

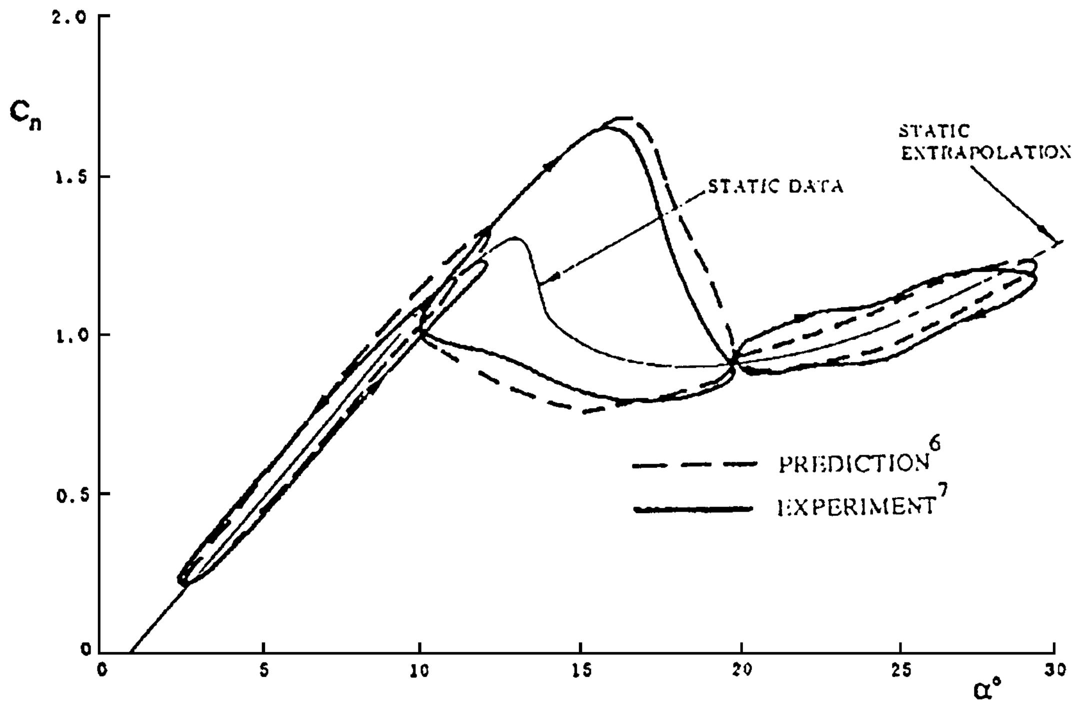

Fig. 1 Predicted and measured dynamic stall characteristics of the VERTOL 23010-1.58 airfoil at $M = 0.4, \bar{\omega} = 0.12$, and $\Delta\theta = 4.85$ deg.

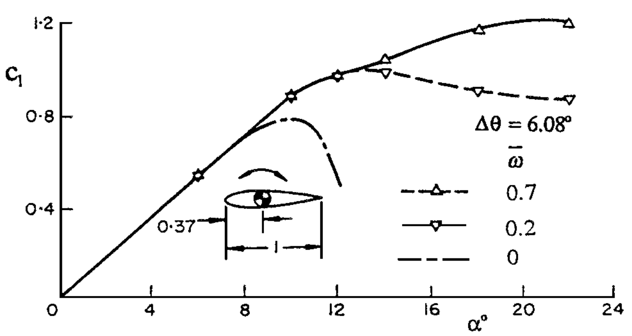

Fig. 2 Time-averaged lift for airfoil describing pitch oscillations at $Re = 10^6$ and $\Delta\theta = 6.08$ deg (Ref. 8).

provides the main contribution to the overshoot of the static stall angle, Eq. (1), and the resulting overshoot of the static lift maximum.

The viscous fluid/motion coupling is fundamentally similar in the three-dimensional case. On a translating cross section of a coning body of revolution (Fig. 6), the stagnation point will again be shifted until the no-slip condition is satisfied, causing the wall immediately adjacent to the flow stagnation line to be subjected to opposing shear stresses. The body is immersed in a rotary flowfield in which the viscous forces contribute to the flow curvature. On the advancing side the surface shear stress is oriented in the same direction as the flow acceleration, determined by the off-surface pressure gradient, whereas on the receding side the shear stresses oppose the flow acceleration. The result is a fuller boundary-layer profile on the advancing side that will make the boundary layer more resistant to separation, whereas on the receding side the effect is the opposite.

As in the two-dimensional case where the dynamic stall behavior cannot be explained by the accelerated flow effect alone, the three-dimensional flow curvature effects cannot explain the flow asymmetries resulting from the coning motion of a body of revolution at high angles of attack. The dramatic effect on the crossflow separation can only be explained by the coning-induced viscous flow effects, which impart momentum to the boundary layer to produce the observed large effects on flow separation. Thus, the flow mechanisms that give rise to the dynamic lift overshoot on the two-dimensional airfoil and those that cause the prospin forces on a coning body of revolution are fundamentally the same. This is demonstrated by the experimental results for a cone cylinder in self-induced coning at $\alpha = 45$ deg (Refs. 15 and 16) (Fig. 7). As the flow conditions near the stagnation point on the coning model at high alpha are similar to those on a rotating circular cylinder, the assumption can be made that the effect of the moving surface on the boundary-layer formation will be similar in the two cases. The prediction[16] was obtained by applying laminar Magnus-lift results for a rotating circular cylinder[5] and applies therefore only to the results for $U_\infty < 10$ m/s in Fig. 7. The discrepancy between prediction and experiment in start-up velocity is the expected result of the bearing friction present in the test,[15] which was not known and, therefore, could not be accounted for in the prediction.[16]

The slender forebody of a combat aircraft will at high angles of attack experience the asymmetric crossflow separation and associated vortex shedding observed on bodies of revolution.[17] The crossflow separation is strongly dependent upon the effective crossflow Reynolds number, which with less than 10% error can be approximated as the Reynolds number based upon the maximum diameter of the forebody.[17] The slender forebody geometries of current combat aircraft usually do not deviate from axisymmetry until well downstream of the apex. It has been established that asymmetric flow separation with associated asymmetric vortex shedding on bodies with pointed noses is initiated at the apex through microasymmetry effects in the case of the static characteristics[17] and through the moving-wall effect for the unsteady aerodynamics.[3] Consequently, the flow physics as depicted in Fig. 6 are representative for most combat aircraft models describing a coning motion, e.g., as in a rotary-rig test.[4] However, the moving-wall effect discussed here is not restricted to axisymmetric configurations. Recent rotary balance tests[18] have shown that the circular approximation of the effective cross section can also be used on nonaxisymmetric bodies, as long as the height-to-width ratio does not exceed unity (with the Reynolds number based on the maximum cross-sectional width).

When the aircraft performs a pitching motion, the crossflow separation process can be simulated using the impulsively started cylinder flow analogy.[19,20] In that case it can be shown[21] that the crossflow acceleration is proportional to $\dot{\alpha} \cos \alpha$. Thus, accelerated flow effects play an important role for a pitching body of revolution. However, for the present case of interest, $\dot{\alpha} = 0$, and no significant accelerated flow effects exist. Instead, as Fig. 6 illustrates, there is a significant

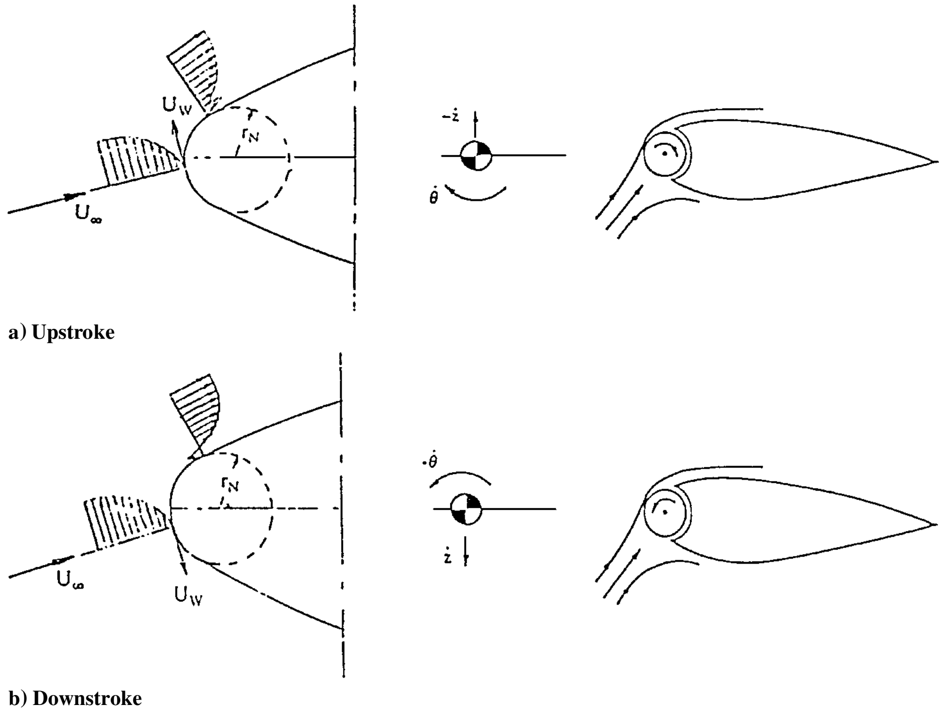

Fig. 3 Leading-edge-jet effect on pitching and plunging airfoils.

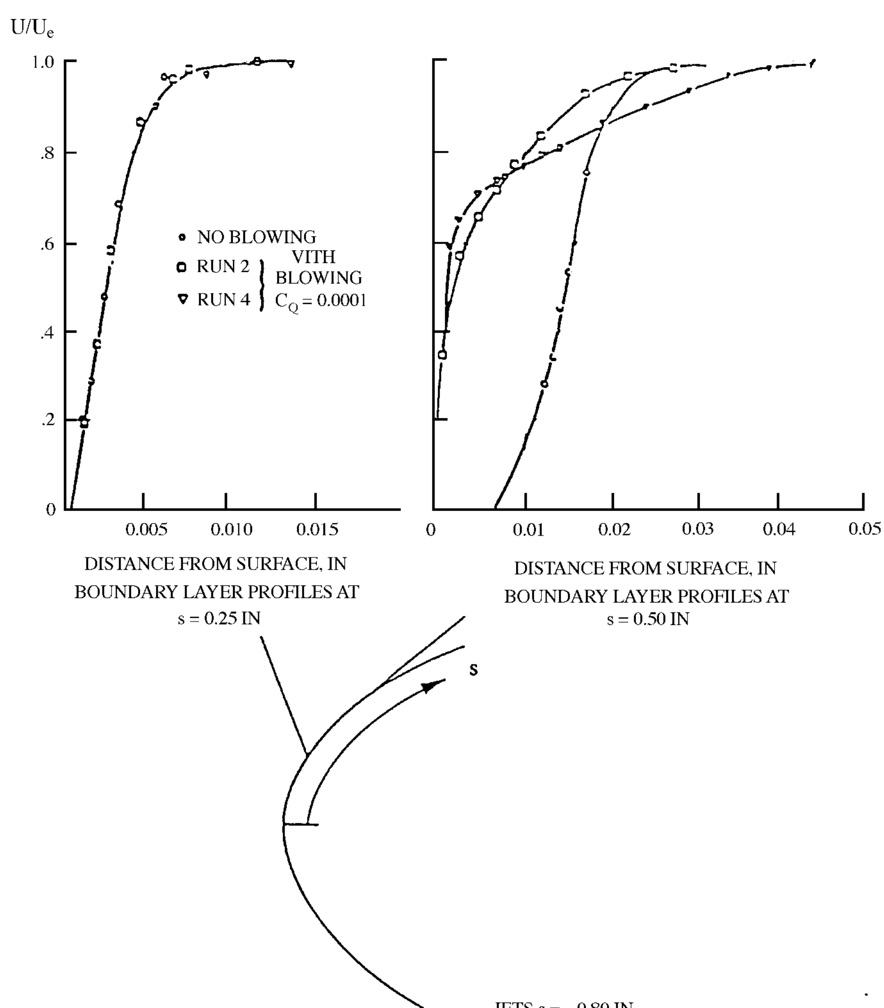

Fig. 4 Effect of leading-edge wall jets on leading-edge stall.[11,12]

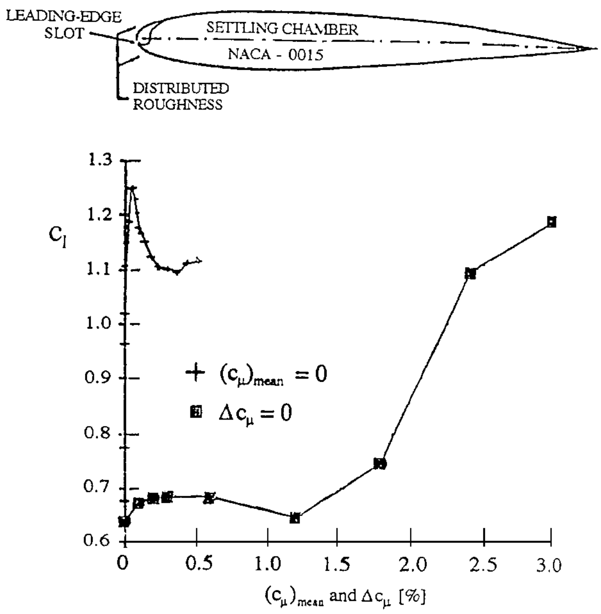

Fig. 5 Effect of steady and oscillating blowing jet on a NACA-0015 airfoil at α = 22 deg.[14]

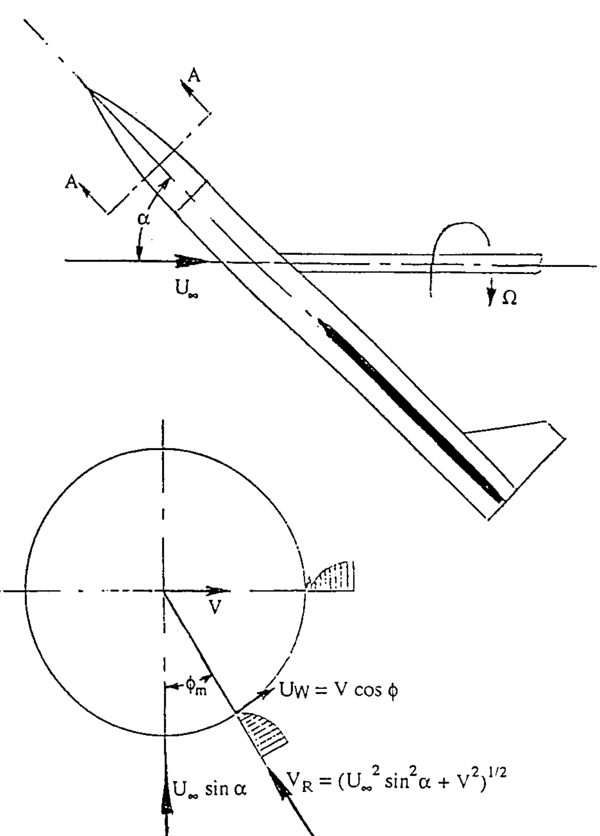

Fig. 6 Forebody flow geometry for a coning aircraft model.

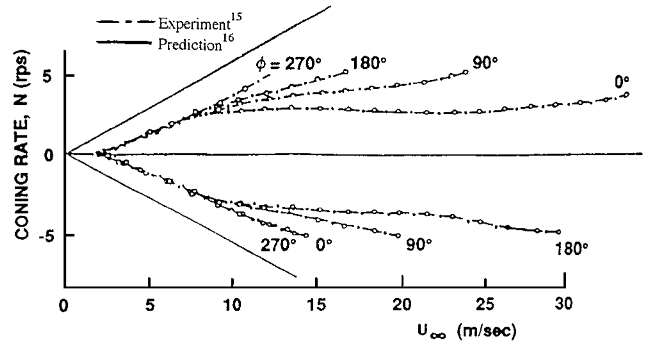

Fig. 7 Moving-wall effects on a cone cylinder in self-induced coning at α = 45 deg (Refs. 15 and 16).

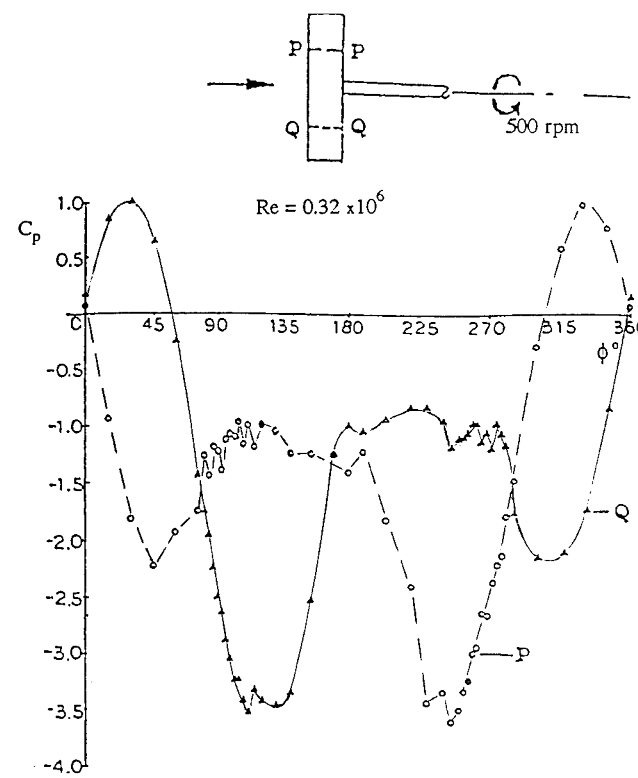

Fig. 8 Cross-sectional pressure distributions on a circular cylinder driven in flat spin.[22]

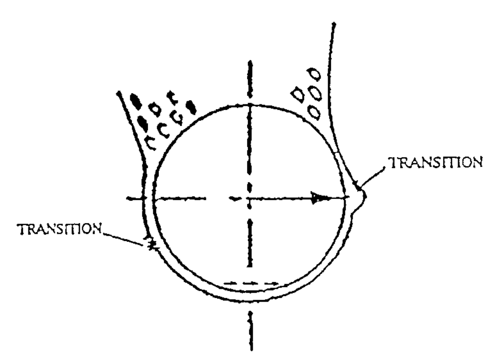

Fig. 9 Conceptual crossflow characteristics on a circular cylinder translating at a critical Reynolds number.

moving-wall effect in the crossflow stagnation region. The figure illustrates how the coning-induced moving-wall effect will generate a wall jet, similar in many aspects to that generated on the airfoil in its plunging motion (Fig. 3a).

The pressure measurements on a circular cylinder driven in flat spin at 500 rpm around the midbody axis at the critical flow conditions existing at $Re = 0.318 \times 10^6$ (Ref. 22 and Fig. 8) demonstrate that moving-wall effects play a dominant role. The crossflow conditions in the flow stagnation region of sections P-P and Q-Q are somewhat similar to those for the plunging airfoil in Fig. 3. At the flow stagnation point $\phi \approx 30$ deg, the moving-wall velocity is 87% of the translational speed of the cross section. The local moving-wall effects produced by the flat-spin motion generated the critical-supercritical flow asymmetry in opposite directions on the two sides of the rotation axis. The stagnation point for section Q-Q in Fig. 8 is at $\phi \approx 30$ deg, corresponding to $\phi = 0$ in the crossflow sketch in Fig. 9. The downstream moving-wall effect delays transition enough to maintain the critical flow separation with its laminar separation bubble. The turbulent boundary layer, reattaching downstream of the bubble,[23] separates at roughly 140-deg azimuth, i. e., at $\phi \approx 140 - 30 = 110$ deg in Fig. 8 for section Q-Q. Figure 9 illustrates how the upstream moving-wall effect has moved the transition forward of the laminar separation bubble, wiping it out on that side. The resulting supercritical separation occurs at roughly 110-deg azimuth.[23] This corresponds to $\phi \approx 360 - 110 + 30 = 280$ deg for section Q-Q in Fig. 8. Considering the data accuracy, the experimental results in Fig. 8 are in good qualitative agreement with the postulated supercritical-critical crossflow separation geometry shown in Fig. 9, which generates a prospin yawing moment. This constitutes an experimental verification of the three-dimensional moving-wall effect on crossflow separation at critical flow conditions. Steady-state flat spin resulted when this prospin moment was balanced by the antispin moment generated by the crossflow drag.[24,25]

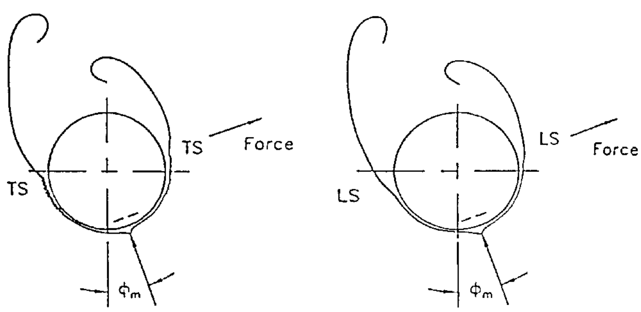

a) Turbulent crossflow b) Laminar crossflow

Fig. 10 Conceptual moving-wall-induced side force on a translating circular cylinder.

Based on this evidence, the suggestion was made in Ref. 1 that the crossflow separation in a section, such as A-A in Fig. 6 on the coning aircraft model, would appear as sketched in Fig. 10. That is, a prospin side force would be generated on the forebody for both turbulent and laminar crossflow conditions. However, when boundary-layer trips were used,[4] the trips at $\phi = \pm 40$ deg from the windward meridian could generate the crossflow characteristics shown in Fig. 11. On the advancing side the trip is close to the flow stagnation point, and there is a long run of favorable pressure gradient downstream of the trip. Thus, even if the trip caused a transition to turbulent flow, relaminarization is likely to occur before flow separation. This was observed to take place on the AGARD WG16 model[4] at $\phi = 53$ deg for $Re = 0.205 \times 10^6$ (Ref. 26). In contrast, on the receding side the trip is farther away from the stagnation point, and the trip could cause transition to turbulent flow conditions before flow separation occurs, resulting in a delay of separation. The end result would be the generation of an antispin force, as illustrated in Fig. 11. This led to the following cautionary statement in the conclusions of Ref. 1: "For all practical purposes it is impossible to fully simulate the conditions at a higher Reynolds number by using boundary layer trips in rotary tests."

Fig. 11 Conceptual effect of boundary-layer trip at $\phi_t = \pm 40$ deg on side force of a translating circular cylinder at subcritical flow conditions.

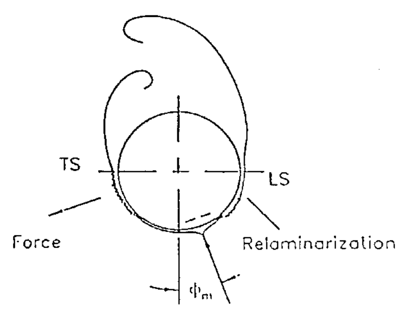

Effect of Flow Unsteadiness

The thorough investigation by Schewe[27] indicated that the establishment of the critical crossflow separation geometry took a time increment Δt that was an order of magnitude larger than the period of the Karman vortex shedding. This is in good agreement with recent pressure measurements on a rotating circular cylinder,[28] which

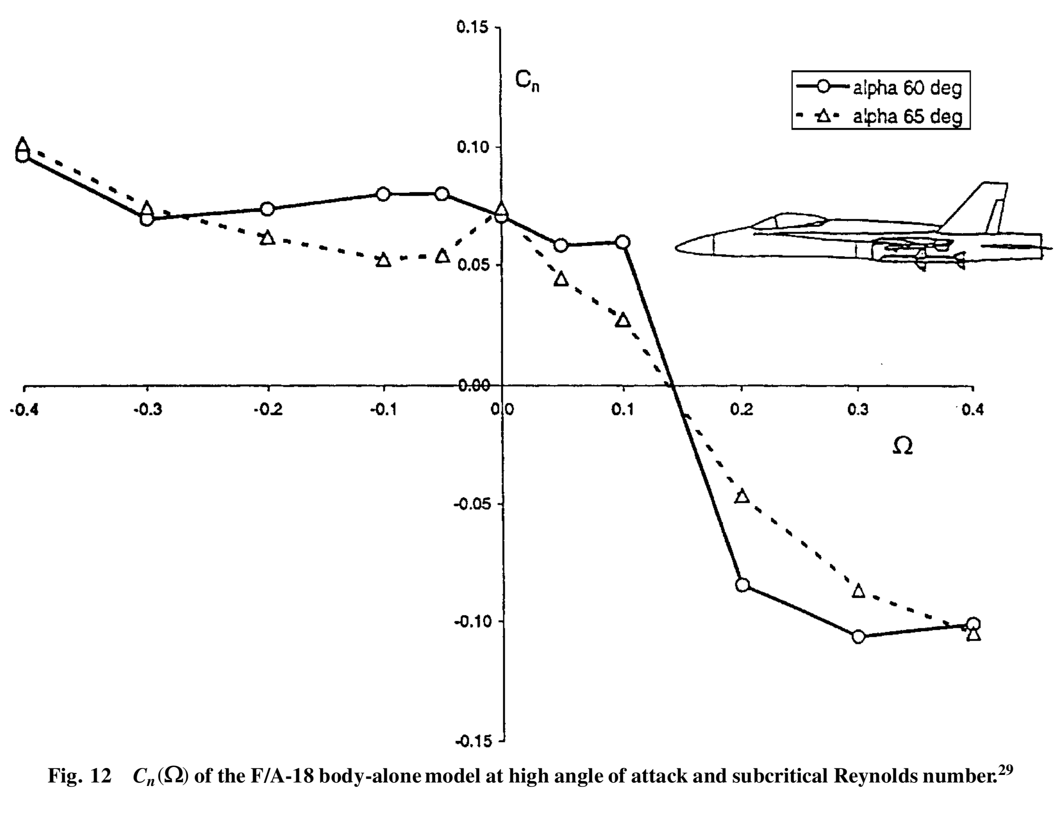

Fig. 12 $C_n(\Omega)$ of the F/A-18 body-alone model at high angle of attack and subcritical Reynolds number.[29]

produced the conclusion that "pressure profiles support previous theories (Ref. 3 here and in Ref. 28) for boundary layer behavior on rotating cylinders." Thus, the high-frequency Karman vortex shedding did not noticeably interfere with the moving-wall effect and the generation of Magnus lift. In the case of the coning motion of a combat aircraft model in rotary rig tests,[1,2] Karman vortex shedding will occur on the slender forebody at high angles of attack, probably already below 60 deg because of the wing-induced upwash. However, as indicated by the experimental results for circular cylinders,[27,28] the high-frequency Karman vortex shedding is not likely to interfere with the moving-wall effect generated at low-frequency combat aircraft maneuvers and should, therefore, not invalidate its application in Refs. 1 and 2.

However, there are cases where flow unsteadiness leads to bifurcation of the time-averaged flow over the forebody and a completely different set of flow physics is generated. Recognition of the presence of threshold values in the coning rate, at which such bifurcation could take place, formed the basis for the analysis in Ref. 2. The vortex breakdown hysteresis on the wing-LEX geometry of the AGARD WG16 generic combat aircraft model[4] is another example of this phenomenon. An illustration of the impact of unsteadiness on the moving-wall effect can be found in the rotary tests of the F/A-18 body alone at a high subcritical Reynolds number (Fig. 12).[29,30] The $C_n(\Omega)$ characteristics show that at 60- and 65-deg angles of attack the bifurcation occurs at $0.1 < \Omega < 0.2$, when the asymmetric crossflow separation and associated vortex system switches between its two stable positions. Close to the bifurcation value of Ω, the associated unsteadiness influences the time-averaged measurements. However, beyond this region, at $-0.3 < \Omega < 0$ and at $\Omega > 0.3$, the proconing $C_n(\Omega)$ trend is evident. This is generated by the moving-wall effect on the translating cross section of the slender fuselage at subcritical crossflow Reynolds numbers (Fig. 10b), acting efficiently in the presence of the static crossflow asymmetry generated by microasymmetry effects.[17] Thus, the moving-wall effect will dominate the aerodynamics of the coning body in the presence of the flow unsteadiness associated with the hysteretic flowfield, except near the bifurcation point(s). The moving-wall effect will also play a role in the generation of the flow unsteadiness. In the tests of the F/A-18 configuration, a detailed investigation of the steady-state hysteresis has been made.[30] The various types of flow unsteadiness that can lead to bifurcation of the time-averaged measurements are of great concern. The possible presence of this danger can only be discovered by performing a methodical search for hysteresis in the static experimental results.

Conclusions

A new interpretation of published experimental results shows that the moving-wall effect is fundamentally the same in two-dimensional and three-dimensional flows, arising from the viscous motion coupling through the boundary layer and being determined by the alignment with the off-surface pressure gradient of the shear stresses caused by the wall motion. The moving-wall effect can be effective in the presence of flow unsteadiness. For a maneuvering combat aircraft this is exemplified by the F/A-18 body, coning at high angles of attack.

Acknowledgment

The authors appreciate the valuable comments made by Murray Tobak.

References

[1]Ericsson, L. E., and Beyers, M. E., "Wind Tunnel Aerodynamics in Rotary Tests of Combat Aircraft Models," *Journal of Aircraft*, Vol. 35, No. 4, 1998, pp. 521–528.

[2]Beyers, M. E., and Ericsson, L. E., "Extraction of Subscale Free-Flight Aerodynamics from Rotary Tests of Combat Aircraft," AIAA Paper 97-0730, Jan. 1997.

[3]Ericsson, L. E., "Moving Wall Effects in Unsteady Flow," *Journal of Aircraft*, Vol. 25, No. 11, 1988, pp. 977–990.

[4]AGARD WG16, "Cooperative Programme on Dynamic Wind Tunnel Experiments for Maneuvering Aircraft," AGARD-AR-305, Oct. 1996.

[5]Swanson, W. M., "The Magnus Effect: A Summary of Investigations to Date," *Journal of Basic Engineering*, Vol. 83, Sept. 1961, pp. 461–470.

[6]Ericsson, L. E., and Reding, J. P., "Unsteady Airfoil Stall, Review and Extension," *Journal of Aircraft*, Vol. 8, No. 7, 1971, pp. 609–616.

[7]Liiva, J., "Unsteady Aerodynamic and Stall Effects on Helicopter Rotor Blade Airfoil Sections," *Journal of Aircraft*, Vol. 6, No. 1, 1969, pp. 46–51.

[8]Halfman, R. L., Johnson, H. C., and Haley, S. M., "Evaluation of High-Angle-of-Attack Aerodynamic-Derivative Data and Stall-Flutter Prediction Techniques," NACA TN 2533, Nov. 1951.

[9]Ericsson, L. E., and Reding, J. P., "Analytic Prediction of Dynamic Stall Characteristics," AIAA Paper 72-682, June 1972.

[10]Ericsson, L. E., "Moving Wall Effect in Relation to Other Dynamic Stall Flow Mechanisms," *Journal of Aircraft*, Vol. 31, No. 6, 1994, pp. 1303–1309.

[11]Wallis, R. A., "Boundary Layer Transition at the Leading Edge of Thin Wings and Its Effect on General Nose Separation," *Advances in Aeronautical Sciences, Proceedings of the Second International Congress in the Aeronautical Sciences*, 1970, pp. 161–184.

[12]Wallis, R. A., " The Turbulent Boundary Layer on the Articulated Nose of a Thin Wing Provided with Air Jets," Research Lab., Aero Note 141, Aeronautical Research Laboratories, Melbourne, Australia, Oct. 1954.

[13]Jones, K. D., and Platzer, M. F., "A Fast Method for the Prediction of Dynamic Stall Onset on Turbomachinery Blades," American Society of Mechanical Engineers, Paper 97-GT-101, June 1997.

[14]Wygnanski, I., and Seifert, A., "The Control of Separation by Periodic Oscillations," AIAA Paper 94-2608, June 1994.

[15]Yoshinaga, T., Tate, A., and Inoue, K., "Coning Motion of Slender Bodies at High Angles of Attack in Low Speed Flow," AIAA Paper 81-1899, Aug. 1981.

[16]Ericsson, L. E., "Prediction of Slender Body Coning Characteristics," *Journal of Spacecraft and Rockets*, Vol. 28, No. 1, 1991, pp. 43–49.

[17]Ericsson, L. E., and Reding, J. P., "Asymmetric Flow Separation and Vortex Shedding on Bodies of Revolution," Progress in Astronautics and Aeronautics, Vol. 141, AIAA, Washington, DC, 1992, pp. 391–452.

[18]Blake, W., and Barnhart, B., "Rotational Aerodynamics of Elliptic Bodies at High Angles of Attack," AIAA Paper 90-0068, Jan. 1990.

[19]Allen, H. J., and Perkins, E. W., "Characteristics of Flow Over Inclined Bodies of Revolution," NACA RM-A50L07, March 1951.

[20]Sarpkaya, T., "Separated Flow About Lifting Bodies and Impulsive Flow About Cylinders," *AIAA Journal*, Vol. 4, No. 3, 1966, pp. 414–426.

[21]Ericsson, L. E., and Beyers, M. E., "Nonlinear Rate and Amplitude Effects on a Generic Combat Aircraft Model," AIAA Paper 98-0409, Jan. 1998.

[22]Kubota, H., Irai, I., and Matsuka, M., "Wind Tunnel Investigations for the Flat Spin of Slender Bodies at High Angles of Attack," *Journal of Spacecraft and Rockets*, Vol. 20, No. 2, 1983, pp. 108–114; also AIAA Paper 82-0054, Jan. 1982.

[23]Achenbach, E., "Influence of Surface Roughness on the Crossflow Around a Circular Cylinder," *Journal of Fluid Mechanics*, Vol. 46, Pt. 2, 1971, pp. 321–335.

[24]Ericsson, L. E., "Flat Spin of Axisymmetric Bodies in the Critical Flow Region," *Journal of Spacecraft and Rockets*, Vol. 24, No. 6, 1987, pp. 532–538.

[25]Ericsson, L. E., and Beyers, M. E., "Flat Spin of a Circular Cylinder," *Journal of Aircraft*, Vol. 33, No. 4, 1996, pp. 722–729.

[26]Beyers, M. E., and Ericsson, L. E., "Aerodynamic Analysis and Interpretation of WG16 Results," AGARD-AR-305, Appendix 4, Oct. 1996.

[27]Schewe, G., "Sensitivity of Transition Phenomena to Small Perturbations in Flow Around a Circular Cylinder," *Journal of Fluid Mechanics*, Vol. 172, 1986, pp. 33–46.

[28]McLaughlin, T. E., Stephen, E. J., and Robinson, M. C., "Pressure Measurements on a Rotating Circular Cylinder," AIAA Paper 91-3265, Sept. 1991.

[29]Hultberg, R., "Low Speed Rotary Aerodynamics of F-18 Configuration for 0 to 90° Angle of Attack-Test Results and Analysis," NASA-CR-3608, Aug. 1984.

[30]Cai, H. J., and Beyers, M. E., "OPLEC Investigation of F/A-18 High-Alpha Aerodynamic Nonlinearities," National Research Council, LTR-A-046, Ottawa, Canada, Nov. 1999.